Experimental investigation of flux motion in exponentially shaped Josephson junctions

G. Carapella,* N. Martucciello, and G. Costabile
INFM Research Unit and Department of Physics "E. R. Caianiello," University of Salerno, via S. Allende, I-84081 Baronissi, Italy
(Received 4 March 2002; published 31 October 2002)

We report an experimental and numerical analysis of exponentially shaped long Josephson junctions with lateral current injection. Quasilinear flux flow branches are observed in the current-voltage characteristic of the junctions in the absence of a magnetic field. A strongly asymmetric response to an applied magnetic field is also exhibited by the junctions. Experimental data are found in agreement with numerical predictions and demonstrate the existence of a geometry-induced potential experienced by the flux quanta in nonuniform width junctions.

DOI: 10.1103/PhysRevB.66.134531 PACS number(s): 74.50.+r

I. INTRODUCTION

In recent years, there have been theoretical studies concerning the possibility of influencing the flux motion in long Josephson junctions by geometry-induced or field-induced potentials. The best known example is the annular junction embedded in a spatially homogeneous magnetic field. In this case,[1] when a spatially homogeneous magnetic field is applied parallel to the junction barrier, a cosinusoidal potential is experienced by a flux quantum trapped in the junction. Here the potential is generated by the spatial variation of the radial component of the magnetic field that in this special geometry exhibits a sinusoidal behavior. As a further example, a field-induced sawtoothlike potential has been recently considered[2] for experimental demonstration[3] of the ratchet effect in annular junctions. Currently, modifications of the annular geometry, such as the heart-shaped geometry,[4] are employed to achieve a field-induced double-well potential for the investigation of fluxon quantum-bit and macroscopic quantum coherence phenomena.

To build up a potential without the help of a magnetic field, the case of a nonuniform junction width has been theoretically addressed in recent years for linear[5–8] as well as for annular[9] geometry. It was shown that a geometry-induced potential originated by the spatial variation of the junction width should be expected. This potential corresponds to a force acting on the fluxon in the direction of the shrinking width. Recently,[10] ordinary Josephson flux-flow oscillators[11,12] have been modified, adding to the classical overlap geometry[13] unbiased pointed tails. This is expected to help the annihilation of the fluxons at the edge of the oscillator, reducing the fine structure of the ordinary velocity-matching step.[11,12,14]

In this paper we experimentally address the existence of the geometrical force in nonuniform width junctions. To do this, we consider an exponentially shaped overlap junction with lateral current injection, i.e., a juntion where the bias current flows in a narrow region of the electrodes near the wide edge. The region where the current is injected acts as a flux quanta generator, also in the absence of a magnetic field, while the unbiased shaped region should accelerate the generated fluxons (or antifluxons). Therefore, if really present, the geometric force should allow us to achieve an essentially unidirectional flux flow in the junction, directed from the wide edge to the narrow edge, without the help of a magnetic field. This dynamical regime is supposed to manifest as a branch in the current-voltage curve of the junction. The occurrence of such branches in the current-voltage curves of shaped junctions we tested provides evidence that such a geometrical force is really exerted upon the flux quanta.

The paper is organized as follows. In Sec. II we specialize the general model[6,7] for a long junction with nonuniform width to our exponentially shaped junction with lateral current injection. In Sec. III the experimental results both in the absence of a magnetic field and in the presence of a magnetic field are presented and discussed with the help of numerical simulations. Finally, main results are summarized in the Conclusions.

II. THEORY

Under some simplifying hypotheses,[6] the model for a long overlap junction with nonuniform width $W(x)=f_1(x)-f_2(x)$ was found as[6,7]

$$\phi_{xx}-\phi_{tt}=\sin\phi+\alpha\phi_t-\frac{W'(x)}{W(x)}\phi_x+\eta_y\frac{W'(x)}{W(x)}-\Gamma(x), \tag{1}$$

with

$$\Gamma(x)=\frac{\eta_x|_{f_2}-\eta_x|_{f_1}}{W(x)}. \tag{2}$$

In Eq. (1), ϕ is the Josephson phase, α is the dissipation parameter, and η_x and η_y are the normalized magnetic fields in the x and y directions, respectively. Space is normalized to the Josephson penetration length λ_J and time to the inverse of the plasma frequency $\omega_J=\overline{c}/\lambda_J$, with $\overline{c}$ the velocity of electromagnetic waves in the junction. For the geometry we report here (see Fig. 1), the total physical length of the junction is $L=L_0+L_S+L_L\gg\lambda_J$, while the width is chosen as

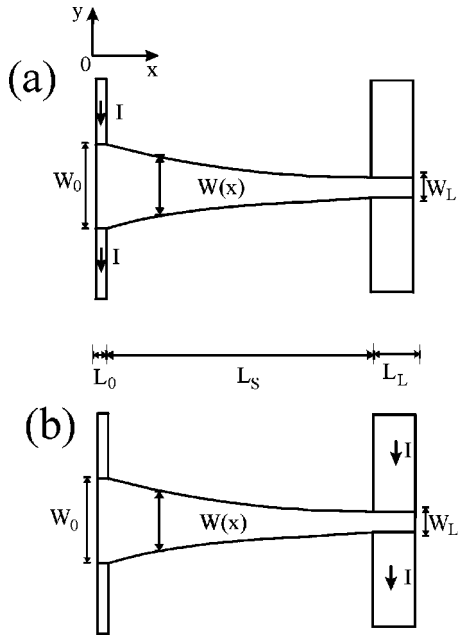

FIG. 1. Exponentially shaped junction with lateral current injection. The current can be fed into the left [(a)] or right [(b)] edge.

$$W(x)=\begin{cases} W_0 & 0<x\leq L_0, \\ W_0\exp\left[\dfrac{1}{L_S}\ln\left(\dfrac{W_L}{W_0}\right)(x-L_0)\right], & L_0<x\leq L_S+L_0, \\ W_L & L_S+L_0<x\leq L. \end{cases} \tag{3}$$

The bias current I can be fed into the left or right edge, as shown in Fig. 1. The bias term $\Gamma(x)$ in Eq. (2) becomes

$$\gamma_A(x)=\begin{cases} \dfrac{IL}{J_0L_0W_0L}\equiv\gamma\dfrac{L}{L_0}, & 0<x\leq L_0, \\ 0, & L_0<x\leq L, \end{cases} \tag{4}$$

for left edge current injection, and

$$\gamma_B(x)=\begin{cases} 0, & 0<x\leq L_S+L_0, \\ \dfrac{IL}{J_0L_LW_LL}\equiv\gamma\dfrac{L}{L_L}, & L_S+L_0<x<L, \end{cases} \tag{5}$$

for right edge current injection. The lengths L_0, L_L, W_0, and W_L are chosen to be shorter than λ_J, and such that $L_LW_L=L_0W_0$, in order to have equal bias areas.

Hence, the model for our exponentially shaped junction becomes

$$\phi_{xx}-\phi_{tt}=\sin\phi+\alpha\phi_t+\lambda\phi_x-\eta\lambda-\gamma_{A,B}(x), \tag{6a}$$

$$\varphi_x(0)=\eta, \tag{6b}$$

$$\varphi_x(l)=\eta, \tag{6c}$$

where $l=L/\lambda_J$, $\lambda=\lambda_J\ln(W_0/W_L)/L_S$, and η accounts for an external magnetic field applied in the y direction. We remark that the chosen geometry turns into to the exponentially shaped in-line geometry[7,8] if the current is injected over a distance L_0 (at the left edge in Fig. 1) much smaller than λ_J. In such a limit, the model becomes

$$\phi_{xx}-\phi_{tt}=\sin\phi+\alpha\phi_t+\lambda\phi_x-\eta\lambda, \tag{7a}$$

$$\varphi_x(0)=\eta-\gamma l, \tag{7b}$$

$$\varphi_x(l)=\eta. \tag{7c}$$

As first noted in Ref. 6, a force that drags fluxons or antifluxons in the direction of the narrowing width is expected for our geometry. In fact, in the absence of a magnetic field ($\eta=0$), for a soliton,

$$\phi(x)=4\arctan\left[\exp\left(\sigma\frac{x-ut}{\sqrt{1-u^2}}\right)\right]$$

in the unbiased region [$\gamma_{A,B}(x)=0$], the following equation of motion can be found from Eqs. (6) in the framework of the perturbative approach:[15]

$$(1-u^2)^{-3/2}\frac{du}{dt}=-\alpha\frac{u}{\sqrt{1-u^2}}+\frac{\lambda}{\sqrt{1-u^2}}. \tag{8}$$

This indicates that, if present, both a fluxon or an antifluxon will experience a force proportional to the shape parameter λ and will be accelerated in the narrowing width direction, i.e., from the left to the right in Fig. 1. From Eq. (8) the stationary velocity of the motion will be $u=\lambda/\alpha$ for $\lambda/\alpha<1$ or the limit velocity $u=1$ for $\lambda/\alpha>1$.

III. NUMERICAL AND EXPERIMENTAL RESULTS

We fabricated $Nb/Al_2O_3/Nb$ junctions with the geometry shown in Fig. 1. The physical dimensions of the junctions were $L=L_0+Ls+L_L=(10+560+40)$ μm, $W_0=40$ μm, and $W_L=10$ μm. For the two junctions we report here the normalized lengths were $l\approx20$ and $l\approx17$, with shape parameters $\lambda\approx0.07$ and $\lambda\approx0.08$, respectively. In the following the behavior of the junctions in the absence of a magnetic field as well as the response to a magnetic field applied along the y direction is discussed.

A. Behavior in the absence of a magnetic field

The current-voltage curve for the junction with $l\approx20$ is reported in Fig. 2. No external magnetic field is applied to the junction. Frame (a) of this figure refers to the case of current injected at the left edge, while frame (b) refers to the case of current injected at the right edge. In both cases an almost linear branch starting from a critical current is observed, but some qualitative difference exists between the two cases. As better seen in Fig. 2(c), when current is injected into the junction at the left edge the branch starts at a lower critical current and is more regular than the branch exhibited when the current is injected at the right edge. This behavior seems to be consistent with the idea that a geometrical force is effectively experienced by the fluxons in this geometry. When current of positive (negative) polarity is injected at the left edge, antifluxons (fluxons) will enucleate

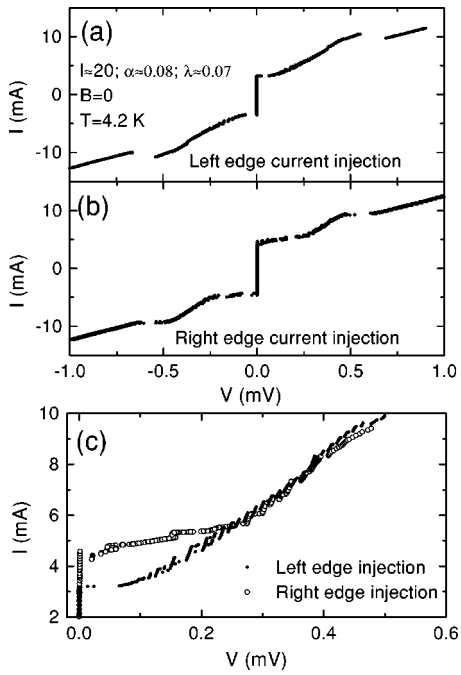

FIG. 2. Current-voltage curve of a junction with left current injection (a) or with right current injection (b) exhibiting quasilinear flux-flow branches. In (c) the flux-flow branch for left current injection is compared with the one achieved for right current injection.

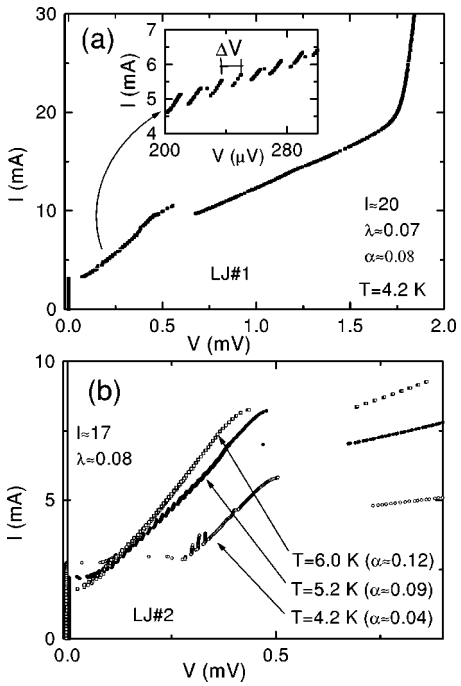

FIG. 3. (a) The current-voltage curve of Fig. 2(a) is replotted on a larger scale. Small steps in the flux-flow branch are shown in the inset. (b) Flux-flow branch of a junction with $\lambda \approx 0.08$ at different temperatures.

at this edge when the current exceeds a threshold value. From Eq. (8), these antifluxons are expected to be accelerated toward the other edge because of the geometrical force, so as to estabilish a steady unidirectional flux motion. Conversely, if the current is injected at the right edge, the antifluxons nucleated at this edge should overcome an opposing force to travel toward the left edge. This should result in an irregular or chaotic flux motion. Moreover, in the left current injection the geometrical force helps to start an antifluxon (or fluxon) motion, corresponding to a nonzero voltage in the *I-V* curve beyond the threshold current. In the case of right current injection such a force opposes the start of the flux motion, and this results into a larger threshold current.

We should remark that the quasilinear branches reported in Fig. 2 could remind one of the displaced linear slope branches sometimes reported for rectangular in-line or overlap geometries.[16–20] However, here the branches are rather regular, very smooth, and they are obtained in the absence of a magnetic field.

In the following we will focus on the case of the left current injection. In Fig. 3(a) the same data of Fig. 2(a) are replotted on a larger scale. As better seen in the inset, the flux-flow branch exhibits a series of small steps spaced by a voltage $\Delta V \approx 15\ \mu$V. The curve closely reminds us of the numerically predicted curve for an exponentially shaped asymmetric in-line junction.[8] The observed voltage spacing is consistent with the spacing of cavity mode resonances calculated from the physical dimensions of the junction, $\Delta V \simeq \Phi_0 \bar{c}/L$. This is to be expected due to the open circuit boundary conditions at the edges. The antifluxons in the chain moving toward the right edge will be reflected as fluxons. If the dissipation α is not too large, the antifluxons can have enough energy to travel toward the left edge as fluxons after the reflection, despite the geometrical force opposing the motion. This mechanism can excite cavity mode resonances. However, for quite large dissipation one expects that the reflected motion would be more and more damped, and the excitation of cavity modes should be consequently damped. In Fig. 3(b) the *I-V* curve of the junction with $l \approx 17$ is plotted for three different temperatures, corresponding to three different α values. As expected, the small steps accounting for the cavity mode resonances are more and more damped as the dissipation (temperature) is increased.

To gain further insight into the flux dynamics in the absence of a magnetic field, we integrated the model, Eqs. (6), with $\eta = 0$ and forcing term $\gamma_A(x)$ defined in Eq. (4). In Fig. 4(a) we show the calculated current-voltage curve for a junction with left edge current injection, having uniform width [$\lambda = 0$ in Eqs. (6)]. This is equivalent to the asymmetric in-line rectangular geometry.[13] As seen in the snapshot showing the instantaneous voltage distribution in the junction, antifluxons are created at the biased edge. However, due to the absence of a force in the unbiased region, the flux motion is not very regular. Here it is only the repulsion between flux quanta that tends to drive the flux toward the right edge. The resulting motion is quite irregular, as well as the calculated ac voltage at the right edge.

In Fig. 4(b) the case of an exponentially shaped width ($\lambda = 0.07$) is considered. In the simulation we used parameters similar to the ones estimated for the experimental curve in Fig. 3(a). As is seen in the snapshot, now the presence of a force in the unbiased region makes the flux motion toward

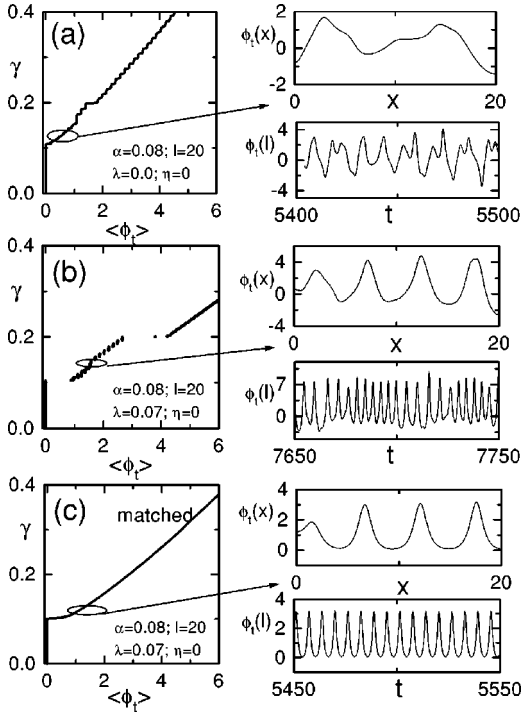

FIG. 4. Calculated current-voltage curve for an unmatched rectangular [(a)], for an unmatched exponentially shaped [(b)], and for a matched exponentially shaped [(c)] junction with lateral current injection. The snapshots shows the instantaneous voltage profiles and the voltage signal at the right edge of the junctions.

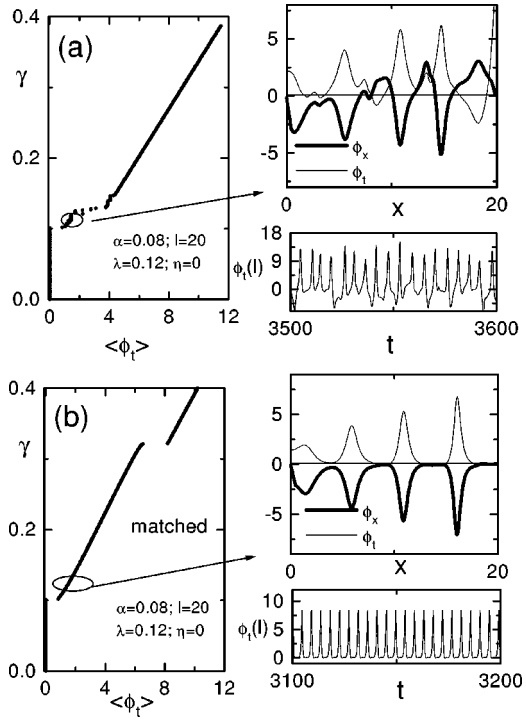

FIG. 5. Calculated current-voltage curve for an unmatched [(a)] and a matched [(b)] exponentially shaped junction with $\lambda=0.12$. The snapshots shows the instantaneous voltage and magnetic field profiles, and the voltage signal at the right edge of the junctions.

the right edge more regular, as well as the voltage signal at the right edge. In the snapshot, four antifluxons occur on the average in the junction for the chosen bias current. By increasing the bias current, more and more antifluxons can be injected in the junction, and the chain becomes more and more twisted. As a consequence, the voltage signal at the right edge becomes less impulsive and approaches a sinusoidal form. When the junction is completely filled with antifluxons, a transition to a new dynamical regime, similar to a laminar phase flow,[8] is established. In the current-voltage curve, this transition corresponds to the switch from the flux-flow branch to the main resistive branch, once a critical current value is reached. As in the experimental curve, the small steps in the calculated flux-flow branch are spaced by π/l, the spacing (in normalized units) expected from cavity mode resonances excited from reflection at the edges.

As said above, the resonances can be damped by increasing the dissipation α. However, another way to achieve the same result is to match the impedance of the fluxon chain with a suitable load z at the right edge. The proper matching can be found,[7,8] indeed, for this geometry, while it is not possible for the rectangular asymmetric in-line geometry. For our exponentially shaped junction the wave impedance is just the stationary velocity we have found above, $-\phi_t/\phi_x = u = \lambda/\alpha$. This should be matched to a load having impedance $z=-\phi_t(l)/\phi_x(l)$. Numerical results for the case of a matched load are shown in Fig. 4(c). As a result of the absence of reflections, the small steps typical of the unmatched case [Fig. 4(b)] disappear and the flux chain exhibits a very smooth motion, and the voltage signal at the matched edge is now clean. This feature makes the exponentially shaped junction interesting as zero field flux flow oscillator.

In Fig. 5 are shown numerical results for a junction with $\lambda/\alpha>1$. For the unmatched case shown in Fig. 5(a) the parameters therein can account for the current-voltage curve at $T=4.2$ K in Fig. 3(b). In both cases $\lambda/\alpha>1$. As said above, in such a case the antifluxons are accelerated toward the asymptotic velocity $u=1$, so that the matching condition becomes $z=1$. In the snapshots shown in Fig. 5(a) and 5(b) we show also the instantaneous magnetic field. Antifluxons in the chain are accelerated and, due to their relativistic nature, they are Lorentz contracted as the asymptotic velocity is approached. As for the case $\lambda/\alpha<1$, the matched junction exhibits a smooth flux-flow branch and the voltage signal at the right edge is very regular.

B. Behavior in the presence of a magnetic field

Due to the lateral current injection and due to the existence of a preferred direction of motion, our exponentially shaped junction is expected to show a behavior in magnetic field even more asymmetric than the asymmetric rectangular in-line geometry. The calculated critical current as a function of the magnetic field is shown in Fig. 6(a) for a junction with $l=20$ and different shape parameters λ. The patterns were obtained integrating Eqs. (6) with $\eta\neq 0$. A quite abrupt decrease of the critical current around $\eta=2$ is found. In normalized units, for this value of the magnetic field a fluxon is generated in the junction. In the junctions with $\lambda\neq 0$ the

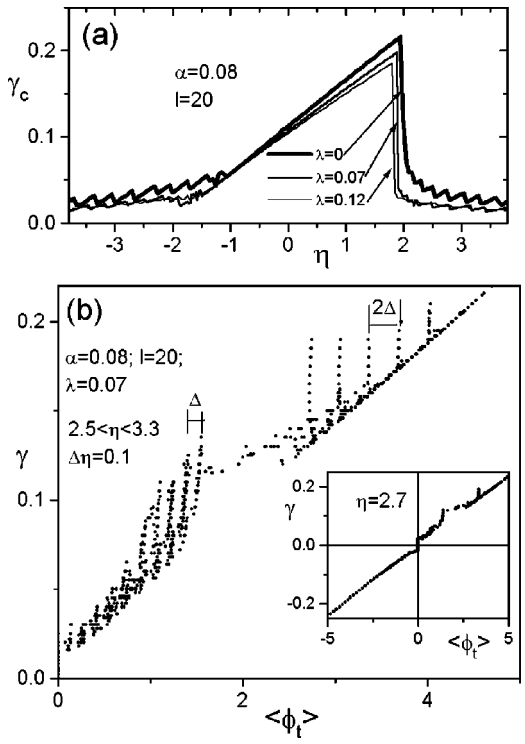

FIG. 6. (a) Calculated magnetic field pattern for a junction with different λ values. (b) Calculated steps induced in the current voltage characteristic of a junction with $\lambda = 0.07$ by a magnetic field varied in the range $2.5 < \eta < 3.3$. In the inset the steps for a given field value are shown.

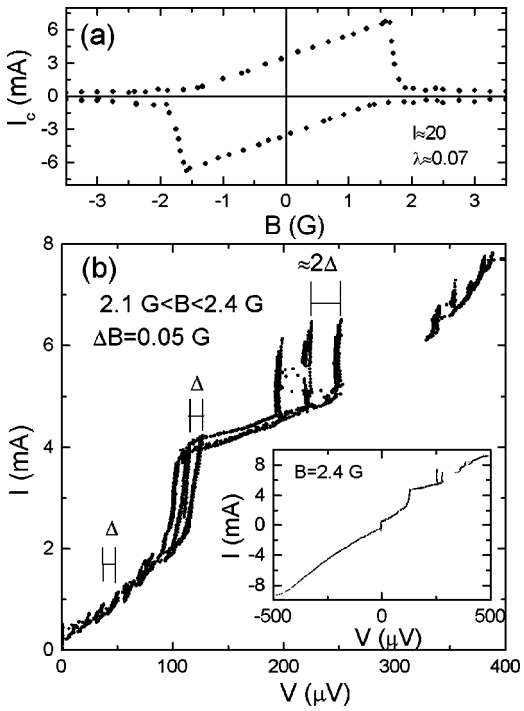

FIG. 7. Measured magnetic field pattern (a) and current steps (b) induced in a junction with $\lambda \approx 0.07$ by a magnetic field slightly larger than the critical field. In the inset the current-voltage curve at B=2.4 G is shown.

magnetic field pattern of the critical current barely exhibits secondary lobes. This indicates that there is little or no flux trapped in this kind of junction, due to the geometrical force dragging the fluxons immediately after their enucleation.

Figure 6(b) gives a global representation of resonance steps calculated for normalized magnetic field values slightly larger than the critical value $\eta = 2$. Such a plot, relative to a junction with $\lambda = 0.07$, is obtained superimposing the curves corresponding to different values of the magnetic field. Two families of steps with two characteristic voltage spacings are obtained. The lower-voltage spacing is the one expected for Fiske mode resonance, $\Delta \sim \pi/l$, and the larger one is about $2\pi/l = 2\Delta$. The family of steps with larger voltage spacing appears in the same current range where the flux-flow branch is recorded in the absence of a magnetic field. From numerical simulations it is seen that these steps with larger voltage spacing consist of cavity mode resonances excited by a fluxon chain and an antifluxon chain moving in opposite directions. In fact, for positive bias current an antifluxon chain moving toward the right edge is generated, while a positive magnetic field generates fluxons. These fluxons are pulled toward the left edge by the Lorentz force associated with the positive bias current at this edge. Antifluxons traveling to the right generate a voltage with positive polarity that adds to the voltage of the fluxons traveling to left. This accounts for the larger voltage spacing observed for the steps of this family.

For negative bias currents, the fluxons generated by the positive magnetic field are pushed toward the right edge by the Lorentz force associated with the negative bias current. Moreover, also the fluxon chain injected at the left edge by the bias current moves to the right, under the action of the geometrical force. The result is that a unidirectional motion toward the right edge tends to be established, with consequent damping of resonant steps originated by cavity mode resonances. As seen in the inset of Fig. 6(b), resonant steps are in fact virtually absent for negative bias current. This peculiarity is observed also for larger magnetic field values. For negative magnetic fields values, the current-voltage curve shows steps for negative bias current, but it does not for positive bias current. In other words, the current-voltage curve is mirrored with respect to the origin when the sign of the magnetic field is reversed.

The behavior of the critical current in magnetic field, summarized in Fig. 6, is found in the experiment (Fig. 7) as asymmetric as predicted. Experimental data are recorded from the junction with $l \approx 20$ and $\lambda \approx 0.07$. In Fig. 7(b) the steps occur for a magnetic field slightly larger than $B_c = 1.75$ G, the critical field of the junction. As in the numerical curves [Fig. 6(b)], two families of steps are also observed in the experimental curves, with the family at lower voltages spaced one half the spacing of the family at higher voltages.

In Fig. 8(a) we report the modification of the flux-flow branch induced by a low magnetic field, i.e., lower than B_c. An asymmetric tuning of the branch is seen. This can be easily understood as follows. We are using strongly left-edge-peaked current injection. In this case the junction can be also described as a shaped aysmmetric in-line junction, i.e., with the model of Eqs. (7). Looking at the vortex generator term $\phi_x(0) = \eta - \gamma l$, one can easily realize that a positive magnetic field cooperates with a negative bias current to

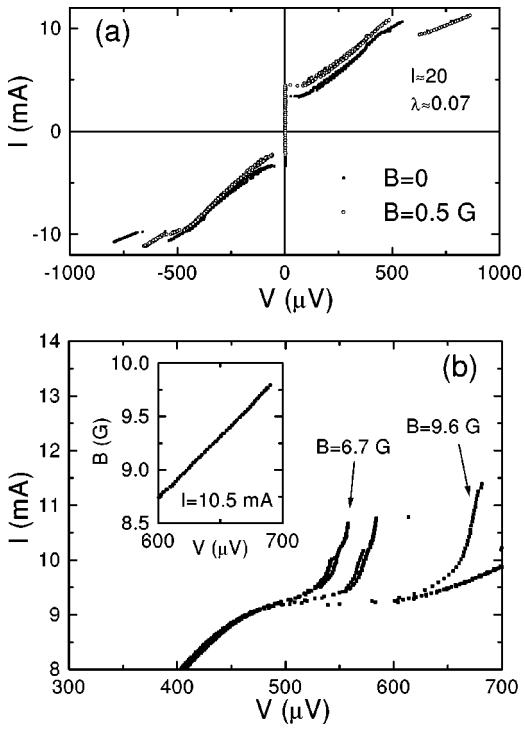

FIG. 8. (a) Modification of the flux-flow branch induced by a magnetic field lower than the critical field. (b) Steps recorded for magnetic fields quite larger than the critical field of the junction. A smooth single step is observed for $B>8$ G. In the inset we show the voltage of the junction biased with a fixed current on the step as a function of the magnetic field.

inject fluxons in the junctions, while such a positive magnetic field opposes a positive current injecting antifluxons into the junction. The result is that, for a given magnitude of the bias current, more vortices are present at negative polarities than at positive polarities, resulting in a voltage at negative polarity larger than the voltage at positive polarity, as it is in fact observed in the experimental curves of Fig. 8(a).

Figure 8(b) shows the steps recorded in the junction for magnetic fields quite larger than B_c. The fine structures accounting for Fiske modes are completely smeared out at $B \approx 9$ G as they merge into a smooth step, similar to the velocity-matching step,[11,12,14] with asymptotic voltage strictly proportional to B. The proportionality between the voltage and magnetic field is shown in the inset for a given bias current. The velocity-matching step is found to exist beyond the current-voltage range of occurrence of the linear flux-flow branch in zero field, i.e., beyond $V=600$ μV (and up to 1500 μV) and $I=9.5$ mA. This is consistent with the observation[14] that the velocity-matching step originates from a quasilinear wave regime in the junction. In our case such a quasilinear background is the laminar phase flow[8] achieved beyond the current range typical of the zero-field flux-flow branch.

IV. CONCLUSIONS

Summarizing, we have experimentally investigated the occurence of dynamical states in exponentially shaped overlap junctions with lateral current injection. In zero magnetic field, the lateral current injection acts as a fluxon or antifluxon chain generator and these chains can be accelerated by the geometrical force originating from the nonuniform width of the junction. The result is that a quite regular flux-flow motion, corresponding to a quasilinear branch in the I-V curve of the junction, can be estabilished in this kind of junction without the help of an external magnetic field. Moreover, numerical simulations show that this kind of motion can be precisely matched to a load, a peculiarity that makes the zero-field flux-flow branch interesting for zero-field flux-flow oscillators. In the presence of a magnetic field a rather asymmetric behavior is exhibited by the junction. For low magnetic fields an asymmetric tuning of the flux-flow branch is observed, for moderated magnetic field ordinary Fiske modes steps are mixed with nonlinear cavity modes steps, and for quite large magnetic fields a single step similar to the velocity-matching step known for uniform width geometries appears in the current-voltage characteristic.

ACKNOWLEDGMENTS

We acknowledge Professor M. Cirillo for providing us with the photolithographic masks we used to fabricate the devices. Fruitful discussions with S. Pagano and C. Nappi, as well as the financial support of MURST COFIN00, are also acknowledged.

*Corresponding author. FAX: +3908965390. Electronic address: giocar@sa.infn.it

[1] N. Grønbech-Jensen, P. S. Lomdahl, and M. R. Samuelsen, Phys. Rev. B **43**, 12 799 (1991).
[2] G. Carapella, Phys. Rev. B **63**, 054515 (2001).
[3] G. Carapella and G. Costabile, Phys. Rev. Lett. **87**, 077002 (2001).
[4] A. Wallraff, Y. Koval, M. Levitchev, M. V. Fistul, and A. V. Ustinov, J. Low Temp. Phys. **118**, 543 (2000).
[5] S. Sakai, M. R. Samuelsen, and O. H. Olsen, Phys. Rev. B **36**, 217 (1987).
[6] S. Pagano, C. Nappi, R. Cristiano, E. Esposito, L. Frunzio, L. Parlato, G. Peluso, G. Pepe, and U. Scotti Di Uccio, in *Nonlinear Superconducting Devices and High T_c Materials*, edited by R. D. Parmentier and N. F. Pedersen (World Scientific, Singapore, 1995).
[7] A. Benabdallah, J. G. Caputo, and A. C. Scott, Phys. Rev. B **54**, 16 139 (1996).
[8] A. Benabdallah, J. G. Caputo, and A. C. Scott, J. Appl. Phys. **88**, 3527 (2000).
[9] E. Goldobin, A. Sterck, and D. Koelle, Phys. Rev. E **63**, 031111 (2001).
[10] V. P. Koshelets, P. N. Dmitriev, A. S. Sobolev, A. L. Pankratov, V. V. Khodos, V. L. Vaks, A. M. Baryshev, P. R. Wesselius, and J. Mygind, Physica C **372-376**, 316 (2002).
[11] T. Nagatsuma, K. Enpuku, K. Sueoka, K. Yoshida, and F. Irie, J. Appl. Phys. **58**, 441 (1985).
[12] V. P. Koshelets, S. V. Shitov, A. V. Shchukin, L. V. Filippenko, J.

Mygind, and A. V. Ustinov, Phys. Rev. B **56**, 5572 (1997).
[13] A. Barone and G. Paternó, *Physics and Applications of the Josephson Effect* (Wiley, New York, 1982).
[14] M. Cirillo, N. Grønbech-Jensen, M. R. Samuelsen, M. Salerno, and G. Verona Rinati, Phys. Rev. B **58**, 12 377 (1998).
[15] D. W. McLaughlin and A. C. Scott, Phys. Rev. A **18**, 1652 (1978).
[16] A. Barone, J. Appl. Phys. **42**, 2747 (1971).
[17] A. C. Scott and W. J. Johnson, Appl. Phys. Lett. **14**, 316 (1969).
[18] S. Pace and U. Gambardella, J. Low Temp. Phys. **62**, 197 (1986).
[19] A. V. Ustinov, H. Kohlstedt, and P. Henne, Phys. Rev. Lett. **77**, 3617 (1996).
[20] P. Cikmacs, M. Cirillo, V. Merlo, and R. Russo, IEEE Trans. Appl. Supercond. **11**, 99 (2001).